2013

Paired Interactions between Kir channels and Tertiapin-Q

Chul Ho Yang
Virginia Commonwealth University

Paired Interactions between Kir channels and Tertiapin-Q

A thesis submitted in partial fulfillment of the requirements for the degree of Master of Science at Virginia Commonwealth University.

by

Chul Ho Yang

BSc. University of Wisconsin, Madison 2010

Thesis Director: DIOMEDES E. LOGOTHETIS
CHAIR, DEPARTMENT OF PHYSIOLOGY AND BIOPHYSICS

Virginia Commonwealth University
Richmond, Virginia
July, 2013

ACKNOWLEDGEMENT

First and foremost, I would like to thank God for giving me wisdom and guidance throughout my life.

I would like to express my sincere gratitude to my thesis mentor, Dr. Diomedes Logothetis for the continuous support of my master study and research, for his patience, motivation, enthusiasm, and immense knowledge. His guidance helped me in all the time of research and writing of this thesis. I would also like to extend my thanks to my committee members, Dr. John Bigbee, Dr. Lei Zhou, and Dr. De Felice who have been supportive throughout this process. Special thanks goes to Dr. Leon Avery, who was willing to participate in my thesis defense committee at the last moment.

I would also like to thank Dr. Shobana Sundaram who has been supportive, encouraging, and funny, Dr. Qiongyao Tang who always has been willing to help me in TEVC recording and statistical analysis, and Dr. Zhe who helped me in the mutagenesis.

My sincere thanks also goes to my colleagues and good friends: Scott Adney, Jason Younkin, Junghoon Ha, Candice Hatcher, and Vasileios Petrou for providing me with tremendous support and enabling me to think critically and carefully about my experiments. They have challenged my thinking and kept filling me with brilliant ideas. I want to thank Heikki and Sophia and all of the other present and past laboratory members of the Logothetis lab who were readily available to help me trouble shooting.

Lastly, and most importantly, I would like to thank my parents, Byung Hee Yang and Hae Ok Lee, my brother, Chul Seung Yang and his family, Seung Hee and Hyun Jik,

and my grandparents, who always encourage, support, and pray for me with trust and unconditional love.

I would like to thank my wife, Ka Yeun Jeong. She was always there cheering me up, stood by me through the good times and bad, and provided me amazing meals all the time. Seohyun Madison Yang, you are the sunshine of daddy' life.

TABLE OF CONTENTS

LIST OF FIGURES

Page

LIST OF ABBREVIATIONS

cRNA	Complementary ribonucleic acid
cDNA	Complementary deoxyribonucleic acid
GIRK	G-protein coupled inwardly rectifying potassium channel
High K^+	High potassium bath solution
Kir	Inwardly rectifying potassium channel
ND96K	High potassium bath solution
ROMK	Renal outer medullary potassium channel
TEVC	Two-electrode voltage clamp
TPN	Tertiapin
TPNQ	Tertiapin derivative with a glutamine residue at position 13

ABSTRACT

Paired Interactions between Kir channels and Tertiapin-Q

by Chul Ho Yang, BSc.

A thesis submitted in partial fulfillment of the requirements for the degree of Master of Science at Virginia Commonwealth University.

Virginia Commonwealth University, 2013

Thesis Director: Diomedes E. Logothetis, Ph.D.

Chair, Department of Physiology and Biophysics

Kir channels serve diverse and important roles throughout the human body and malfunctions of these channels are implicated in various channelopathies. Specific inhibitors for different subtypes of Kir channels are not available. However, Tertiapin-Q (TPNQ), a polypeptide isolated from honey bee venom, differentially inhibits certain subtypes of Kir channels with nanomolar affinity: ROMK1 (Kir1.1) and GIRK1/GIRK4 (Kir3.1/Kir3.4). Modification of TPNQ to increase selectivity for target channels bears great therapeutic potential. The *in silico* studies based on TPNQ-docked channel models, ROMK1_IRK2 (Kir1.1_Kir2.2) and GIRK2 (Kir3.2), predicted specific paired residue interactions and were experimentally validated here. In ROMK1 E123A mutant, the TPNQ sensitivity was decreased by ~2-fold while GIRK2 E127A mutant reduced the TPNQ sensitivity by greater than 10-fold. Also, we could observe the additional effect, ~ 18 fold, of GIRK1 subunits, ~1.7 fold, and E127A mutation, ~10 fold, on the TPNQ sensitivity in the heteromeric mutant channel, GIRK1/GIRK2 E152D_E127A as compared with the homomeric GIRK2 E152D. Finally, we introduced the Kir3.2 E152D mutant as a good representative of wild-type behavior particularly for the TPNQ study. Overall, this type of structure-function studies suggests an efficient and cost effective way toward design and development of specific Kir channel blockers by targeting on specific paired interactions between TPNQ and the Kir channels.

INTRODUCTION

Ion channels are macromolecular transmembrane protein complexes that facilitate the ion movement across the membrane lipid bilayer. They are essential to all kinds of living organisms and are highly conserved from prokaryotes to mammals. The net ion movement across membranes serves many biological functions such as regulating the membrane potential, osmotic balance, and pH. Moreover, their activity has been known to contribute to cellular homeostasis and maintenance of health in many areas of the human body. More than 40 different channelopathies had been identified up to 5 years ago, and modulating channel activity by drugs is widely used to treat channelopathies (Cannon, 2007). Thus, ion channels are one of the largest class of proteins intensely investigated by pharmaceutical industries.

In this study, we are focusing on the inwardly rectifying K^+ (Kir) channels, first identified half a century ago (Katz, 1949). cDNAs of the first two Kir channels, Kir1.1 (ROMK1) and Kir2.1 (IRK1), were isolated by expression-cloning techniques in 1993 (Kubo, 1993; Ho, 1993). The major biological roles of Kir channels are to maintain the resting membrane potential and to regulate the action potential duration in electrically excitable cells such as cardiac muscle (Sakmann, 1983), but some Kir channels also play vital roles in other types of tissues such as ROMK1 in kidney. Their defining characteristic, inward rectification is known to be due to the block of outward K^+ flux by intracellular substances such as Mg^{2+} and polyamines (Lopatin, 1995; Matsuda, 1987). The common basic building block of all Kir channels consists of two membrane spanning domains (M1 and M2) linked by a highly conserved extracellular pore forming region (P) and cytoplasmic amino (N)- and carboxy (C)- terminal domains (Figure 1A). The functional Kir channels are composed of four such subunits as a tetrameric complex (Yang, 1995). The tetrameric complex can be formed either by association of homomeric or heteromeric subunits. So far, 15 Kir subunit genes have been identified and classified into seven subfamilies, also categorized into four functional groups.

Fig. 1

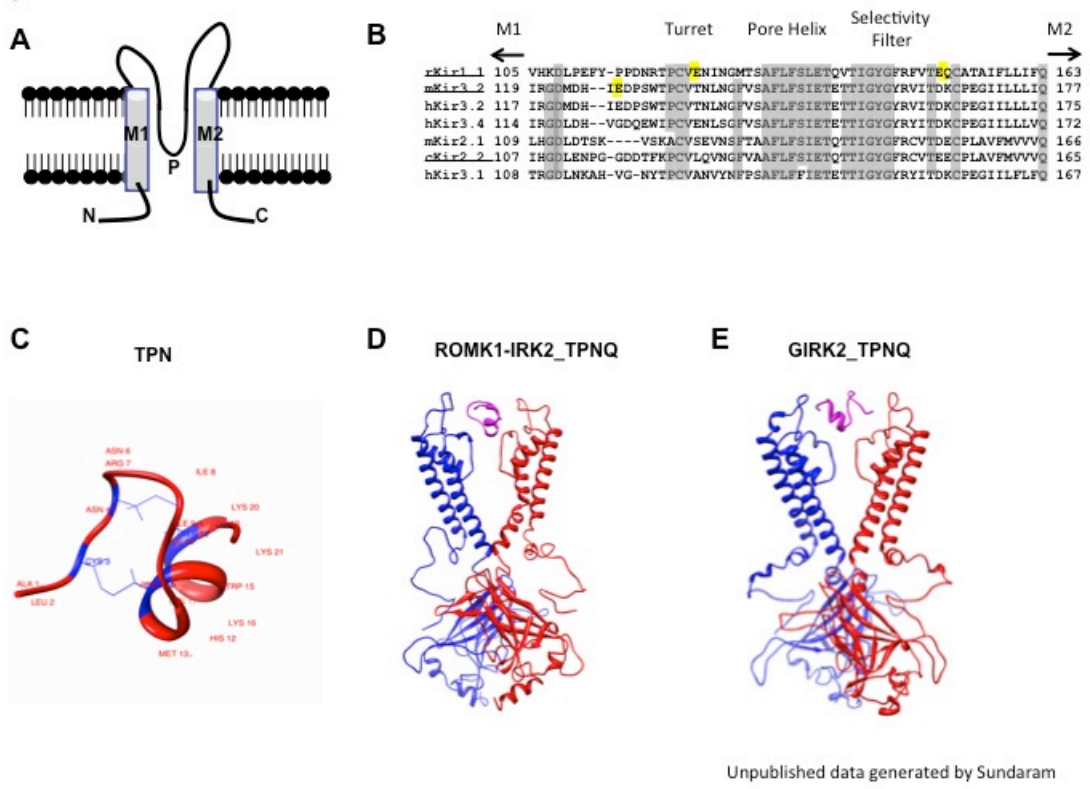

Figure 1. Structural details of Kir channels and channel blocker TPNQ A. Topology of Kir in cartoon representation where, M1 and M2 are the outer and inner transmembrane helices respectively, and P is the pore helix. N and C indicate the N- and C-termini regions of the Kir. **B.** Sequence alignment of 3 TPN-sensitive Kir channels (Kir1.1 or ROMK1, 2 isoforms of Kir3.2 or GIRK2 and Kir3.4 or GIRK4) and 3 TPN-insensitive Kir channels (Kir3.1 or GIRK1, Kir2.2 or IRK2, and Kir2.1 or IRK1) (M1 to M2 linker alignment is shown). The grey regions are conserved regions of Kir channels and the yellow highlighted residues are predicted to be important in the interactions of ROMK1 with TPNQ. The underlined labels are those for which we have either a homology model or a crystal structure. **C.** NMR structural model *(Xu and Nelson, 1993*) of TPN showing the 21 residues and the two-disulphide (3-14; 5-18) linkages from the RCSB protein data bank: 1TER (www.rcsb.org). **D.** TPNQ docked chimeric ROMK1_IRK2 tetrameric channel based on the cKir2.2 crystal structure (*Tao et al., 2009*), **(E)** TPNQ docked GIRK2 tetrameric channel (*Whorton et al., 2011*). Only two subunits of the tetrameric channel are shown for clarity. *This figure was generated by Dr. Sundaram (Sundaram et al., In Preparation).*

In terms of their physiological functions, Kir channels serve diverse and important roles throughout the human body and malfunctions of these channels are implicated in various diseases. For example, Kir1.0, also called ROMK, is predominantly expressed in the kidney and is important in maintaining K^+ homeostasis. Genetic defects of this channel can lead to type II Barter's syndrome with volume depletion and hypotension (Simon, 1996). Kir 3 or G-protein coupled inward rectifier (GIRK) channels are expressed primarily in the brain and heart as either homo- or hetero- tetrameric complexes. In brain where all of GIRK1-GIRK4 are expressed, activation of GIRK channels is involved in the inhibitory actions of various neurotransmitters such as GABA, ACh, and opioid peptides, and mice lacking GIRK2 are known to be more susceptible in developing seizures (Abraham, 1999). Moreover, a heterotetramer of GIRK1/GIRK4 forms the K_{ACh} channel, which mediates vagal control of pacemaker activity (Krapivinsky, 1995). Therefore, specific inhibitors for different subtypes of Kir channels would be very useful for studying their physiological functions and also for designing drugs to treat channelopathies. However, no Kir subtype specific inhibitors are available.

To date, tertiapin (TPN) is the only reported nanomolar-affinity inhibitor that differentially inhibits certain subtypes of Kir channels, such as Kir1.1 or ROMK1 (K_d = 1~2.5 nM) (Ho, 1993; Jin and Lu, 1998), heteromeric Kir3.1/Kir3.4 or GIRK1/GIRK4 (K_d = 10 nM) (Kubo, 1993; Dascal, 1993; Krapivinsky, 1995). Kir2.1 or IRK1 on the other hand have much lower affinity for this peptide toxin (K_d = 2 μM) (Jin and Lu, 1998). TPN, isolated from the honey bee venom, is a small compact protein composed of 21 amino acids (Gauldie et al., 1976; Ovchinikov et al., 1980). Its C-terminal half forms an α-helix, while its N-terminal half forms an extended structure. Two disulfide bonds hold these two structures together (Xu and Nelson, 1993) (Fig. 1C). The methionine residue in position 13 is easily oxidized, and a glutamine mutation at this position prevents oxidation and is more stable. Tertiapin-Q or TPNQ shows no functional differences from the native TPN and exhibits an even higher selectivity (Jin and Lu, 1999).

TPN binds to the channel in one to one stoichiometry, so that one TPN peptide interacts with the Kir channel that is composed of 4 subunits (Jin et al., 1999). The

blocking effect of TPN is sensitive to pH, such that alkaline pH reduces the affinity between the toxin and Kir1.1 (Ramu et al., 2001). In addition, alanine scanning mutagenesis studies on Kir1.1 and TPNQ have shown that the C-terminal α-helix of TPNQ binds to the external vestibule of the K^+ conduction pore formed by the M1-M2 linker (Jin et al., 1999). This is also inferred from the chimeric studies by Lu's group that transferring the M1-M2 linker of a TPNQ sensitive channel, Kir1.1, to a non-sensitive channel, Kir2.1, confers TPN sensitivity to the chimeric channel (Ramu et al., 2004).

Motivated by the above chimeric studies and the availability of Kir2.2 or IRK2 crystal structure (Tao et al., 2009) which is also TPNQ insensitive, Dr. Shobana Sundaram in our lab built a computational chimeric model by transplanting the M1-M2 linker of Kir1.1 in the background of Kir2.2 (Fig. 1D). With this chimeric model, Dr. Sundaram simulated an alanine scanning mutagenesis *in silico* and was able to regenerate the similar trend of the experimental data, which illustrates the changes in the binding interaction between channel and the toxin, shown by the Lu's group (Jin et al., 1999). Moreover, while Lu's data only show how one mutation affects function by changing macromolecular interactions (whole channel and toxin interactions), our *in silico* studies could quantify the energies involved for each channel-toxin interaction pair. Namely, it can specifically identify the toxin and channel interacting residues and quantify their interaction energy (Fig. 2A).

Dr. Sundaram's simulations and calculations on overall energy of interactions between TPNQ and ROMK1 chimera were in close agreement with the experimental data from Zhe Lu's lab and her calculations of specific pairwise interactions of ROMK1 chimera with TPNQ residues showed direct interactions between residues in the channel and the toxin (Fig. 2A). By using mutagenesis and whole-cell current recording with two-electrode voltage clamp (TEVC), we validated the predictions of the paired interactions to see how much mutation of the predicted residues, E123A and E151A, could affect TPNQ sensitivity. In addition, since the crystal structure of GIRK2 had been recently determined by Mackinnon's group (Whorton, 2011), we performed similar *in silico* studies on TPNQ docked GIRK2 model (Fig. 1E; Fig. 2B) and validated them using the same approach used for the Kir1.1 chimeric model. Our study suggests that differences in

the interaction energies can guide the design of a specific TPN blocker for the channel of interest in an efficient and cost effective manner.

Fig. 2

A

TPNQ	ROMK1-IRK2 chimera	Subunit	Energy (kcal)
His12	Tyr144	A	-20.8
	Gly145	B&C	-7.3
Gln13	Tyr144	A	-6.3
	Phe146	A	-16.3
	Glu123	C	-15.4
	Phe148	C	-7.2
Lys16	Glu123	C	-104.7
	Asn124	C	-9.8
	Phe146	C	-19.5
Lys17	Glu123	C	-150.2
	Tyr144	C	-1.2
	Phe146	A	-4.0
	Glu151	C	-132.5
Lys20	Tyr113	C	-16.3
Lys21	Phe112	B	-23.6
	Tyr113	B	-10.3
	Pro114	B	-3.8
	Glu123	B	-55.4

B

TPNQ	mGIRK2	Subunit	Energy (kCal)
Arg7	Glu127	D	-142.3
	Asp128	D	-10.9
	Thr132	D	-7.9
His12	Tyr157	A,B,C&D	-9.2
	Gly158	A,B,C&D	-10.4
Gln13	Tyr136	A	-14.5
	Asn137	A	-8.2
	Tyr159	A	-10.3
Lys16	Glu127	C	-145.7
	Thr132	C	-6.9
	Tyr159	C	-5.9
Lys17	Ile126	A	-7.9
	Glu127	A	-86.6
	Asp128	A	-5.4
	Thr132	C	-4.3
	Tyr159		-18.8
Lys20	Ile126	C	-7.6
	Glu127	C	-135.5
	Asn137	C	-6.3
Lys21	Glu127	B	-39.7
	Pro129	B	-1.5

Unpublished data generated by Sundaram

Figure 2. Studies on paired interacting residues between TPNQ and A. ROMK1_IRK2 chimeric channel **B.** GIRK2 channel. The list of interacting residue pairs between TPNQ and the subunits of the channel and their interaction energies in Kcal. The yellow color highlights the residues of TPNQ and the channel and the highest interaction energies. *This figure was generated by Dr. Sundaram (Sundaram et al., In Preparation).*

MATERIALS AND METHODS

Characterization of channel mutants in the *Xenopus laevis* oocyte system and their interaction with TPNQ were studied experimentally using the two-electrode voltage clamp (TEVC) technique.

In vitro transcription of cRNAs

cDNA constructs of Kir1.1, Kir3.2, Kir3.2 E152D, $G\beta_1$, and $G\gamma_2$ had previously been subcloned into oocyte expression vectors, pGEM-HE (Kir1.1, $G\beta_1$, and $G\gamma_2$) or pXOOM (Kir3.2 and Kir3.2 E152D) by previous laboratory members in order to generate transcripts for expression in *Xenopus laevis* oocytes. The constructs were amplified using supercompetent XL1-Blue *E. coli* (Stratagene, La Jolla, CA) and isolated using a miniprep kit (Fermentas, Glen Burnie, MD).

Prior to cRNA *in vitro* transcription, amplified cDNA subcloned vectors were linearized with *Nhe*I (Kir1.1, $G\beta_1$, and $G\gamma_2$) or *Xho*1 (Kir3.2 and Kir3.2 E152D) digestion overnight at 37°C. cRNAs were *in vitro* transcribed using T7 polymerase (Ambion, Austin, TX). cRNA concentration was quantified by optical density.

Xenopus laevis oocyte injection

Xenopus oocytes were surgically extracted, dissociated and defolliculated by collagenase treatment, then microinjected with 50 nl of a water solution containing the desired cRNAs. The homotetramer constructs used in this study were injected to achieve 10 ng/oocyte (Kir3.2 wild-type, Kir3.2E127A, Kir3.2E152D, and Kir3.2E152D_E127A) or 1 ng/oocyte (Kir1.1 wild-type, Kir1.1E123A, and Kir1.1E151A). Heterotetramer constructs used in this study were coinjected to achieve 2 ng/oocyte (Kir3.1/Kir3.2 wild-type, Kir3.1/Kir3.2 E127A, Kir3.1/Kir3.2 E152D, and Kir3.1/Kir3.2 E152D_E127A) or 1 ng/oocyte (Kir1.1/Kir1.1 E123A and Kir1.1/Kir1.1 E151A) for each subtype. For studies involving $G\beta\gamma$, cRNAs of each subunit were coinjected to achieve 2 ng/oocyte. Oocytes were incubated for 1-3 days at 18 °C.

Injection pipettes were made from borosilicate glass (WPI, Saratosa, FL) using a Sutter P-97 microelectrode puller and were manually cut to produce tips of ~12 mm in diameter.

Mutagenesis

cDNAs for Kir1.1, Kir3.2, and Kir3.2 E152D were already subcloned into an oocyte expression vector, pGEM-HE or pXOOM. Desired mutations were introduced by the commercial Quickchange (Agilent Technologies) method. Briefly, complimentary primers containing and centered about the desired mutation were designed. PCR was carried out using the pfu polymerase and was allowed to cycle only 18 times to avoid errors. All mutants were confirmed by DNA sequencing (Genewiz).

Electrophysiology

Whole-cell recordings were made 24-30 hours (Kir1.1 channels) or 72-80 hours (Kir3.2 channels) after cRNA injection using conventional two-electrode voltage clamp with a GeneClamp 500 amplifier (Axon Instruments). Agarose cushion microelectrodes, filled with 1% agarose in 3 M KCl to prevent leakage of KCl into oocytes, were used with resistances between 0.1 and 1.0 MΩ. All channel currents were recorded in high potassium (ND96K) solution.

The membrane was held at the equilibrium potential, namely at 0 mV. In order to elicit current through the channel, the membrane voltage was stepped to -90 mV and then to +90 mV for one-second intervals. Current at -90 mv was recorded. Barium-sensitive basal currents were defined as the difference between the steady-state currents, while perfusing high potassium (High K^+ or ND96K) solution, and the same solution containing 3mM barium chloride solution. 3 mM barium chloride containing ND96K solution was used for complete block of the Kir currents. Leak currents were considered as the remaining inward currents after exposure to 3 mM barium chloride and subtracted from the total currents measured in High K^+ solution and each TPNQ concentration. Various concentrations of TPNQ were diluted in ND96K and oocytes were perfused with ND96K with or without TPNQ.

The ND96K solution contained: 91mM KCl, 1mM NaCl, 1mM MgCl2, 5mM KOH/HEPES, pH 7.4. The Barium solution consisted of ND96K + 3mM $BaCl_2$. 4-12 oocytes from the same batch were recorded for each TPNQ concentration and the experiments were repeated in at least two batches.

Statistical analysis

All current values in response to 100 ms steps at -90 mV were obtained using Clampfit 9.2 (Molecular Devices, Sunnyvale, CA) and transferred to Excel software (Microsoft, Albuquerque, NM). For each oocyte, 10 data points of the steady-state currents in High K^+ solution, each TPNQ concentration, and 3 mM barium chloride were selected and averaged and then subtracted from the leak currents, except for the currents in 3 mM barium chloride, used to obtain the basal current in ND96K with or without TPNQ. Then, each mean current for the corresponding TPNQ concentrations was normalized by dividing it by the maximal basal current in ND96K without TPNQ. These mean currents were averaged again with other mean currents at the same TPNQ concentration obtained from other oocytes from the same and different batches. The mean current values for each TPNQ concentration with the standard error of the mean (SEM) were transferred into MicroCal Origin Lab and plotted and fitted with a non-linear Growth/Decay/Sigmoidal Curve governed by the Hill function. The Hill function is given by the equation: y = Start + (End - Start)*x^h/(K^h+x^h)). Start is where the curve starts, fixed to 1, and End is where it ends, fixed to 0. x is the TPNQ concentration. K is approximated as the IC_{50} for the binding reaction. h is the Hill coefficient. $n \geq 4$ experiments were used for estimating each data point in the dose-response curve. Error bars in the figures represent standard error. The standard deviations for each data set were divided by the square root of the number of recordings to get the standard errors. The two-sample t test (ROMK1: n= 13 for wild-type, 12 for E123A, 9 for E123A coinjected, and 12 for E151A coinjected, GIRK2: n= 11 for wild-type, 13 for E152D, 13 for GIRK1/GIRK2, 12 for GIRK1/GIRK2 E152D, 11 for GIRK2 E152D_E127A, 9 for GIRK1/GIRK2 E152D_E127A) was used to assess statistical significance.

RESULTS

TPNQ Sensitivities of ROMK1 (Kir1.1) Wild-type Channel

We first examined the apparent affinity of ROMK1 (Kir1.1) for TPNQ in order to compare our results to previously published work. *Xenopus* oocytes were injected with *in vitro* transcribed rat ROMK1 cRNA, and membrane currents were recorded 24-30 hours later using two-electrode voltage clamp (TEVC). In symmetrical 96 mM potassium solutions, ND96K (High K^+), the membrane was held at the equilibrium potential, namely at 0 mV. In order to elicit current through the channel, the membrane voltage was stepped to -90 mV and then to +90 mV for one-second intervals. This protocol allowed us to monitor the characteristic rectification of Kir1.1 and immediately detect changes in leak currents, the remaining inward currents after exposure to 3 mM barium chloride. Various concentrations of TPNQ were diluted in ND96K and oocytes were perfused with ND96K with or without TPNQ. 3 mM Barium Chloride in ND96K solution was used for complete block of Kir1.1 currents.

Each solution was perfused until the current reached a steady state. In agreement with previous studies by Zhe Lu's group (Jin and Lu, 1998; Ramu et al., 2004), we found ROMK1 to be the most sensitive channel to TPNQ. In our hands, ROMK1 showed an IC_{50} value of 8.07 nM ± SEM, which was used as our control to compare with other mutant channels.

Effects of ROMK1 Mutations on TPNQ sensitivity

As predicted by *in silico* studies in Fig. 2A, we selected residues to mutate that showed the highest interaction energy values: Glutamate 123 and 151. Glutamate 123 from two different subunits interacts with Lys 16, 17, and 21 on TPNQ, and Glutamate 151 from one subunit interacts with Lys 17 on TPNQ.

Fig. 3 shows the current traces of ROMK1 wild-type and its mutant channels, E123A and E151A, recorded in the presence and the absence of 10 nM TPNQ. IC_{50} values were obtained using nonlinear curve fitting (Hill equation) based on the plots of the fraction of unblocked currents against the concentration of TPNQ, as illustrated for

the inhibition of ROMK1 and its mutant channels by TPNQ (Fig. 4A). The E123A mutation in ROMK1 significantly increased the IC_{50} by more than 2-fold as compared to the wild-type, which supports our computational prediction that the E123A mutation should cause a decrease in TPNQ sensitivity of ROMK1 channel (Fig. 4B) and is consistent with previous reports (Jin et al., 1999).

ROMK1 with the E151A mutation did not express any detectable ionic currents (Fig. 4B), consistent with results from Zhe Lu's group (Jin et al., 1999). Thus, we coinjected the E151A mutant cRNA with wild-type cRNA in one to one ratio to test whether coexpression of heterotetramers between mutant and wild-type shifted the IC_{50} of the wild-type channel. Coinjected E151A mutant channels showed measurable ionic currents, approximately -19 μA, with less TPNQ sensitivity than that of the wild-type homomeric channels, (Fig. 3C and Fig. 4B).

In order to compare the effect of the two mutations on the channel interaction with TPNQ under identical conditions, a similar coinjection method was also conducted with the E123A mutant channels. Since E123 has a greater number of high energy interactions with TPNQ residues than E151, we expected a greater decrease in TPNQ sensitivity of ROMK1 by the E123A mutation than the E151A. However, our results contradicted with our expectations. The coinjected E123A mutant channels did not show a statistically significant difference from the coinjected E151A mutant channels in TPNQ sensitivity (Fig. 3B). Furthermore, this coinjection method shows a titration of IC_{50} values between wild-type and mutant channels, as illustrated by the E123A/wild-type mixtures (Fig. 4A and B).

Fig. 3

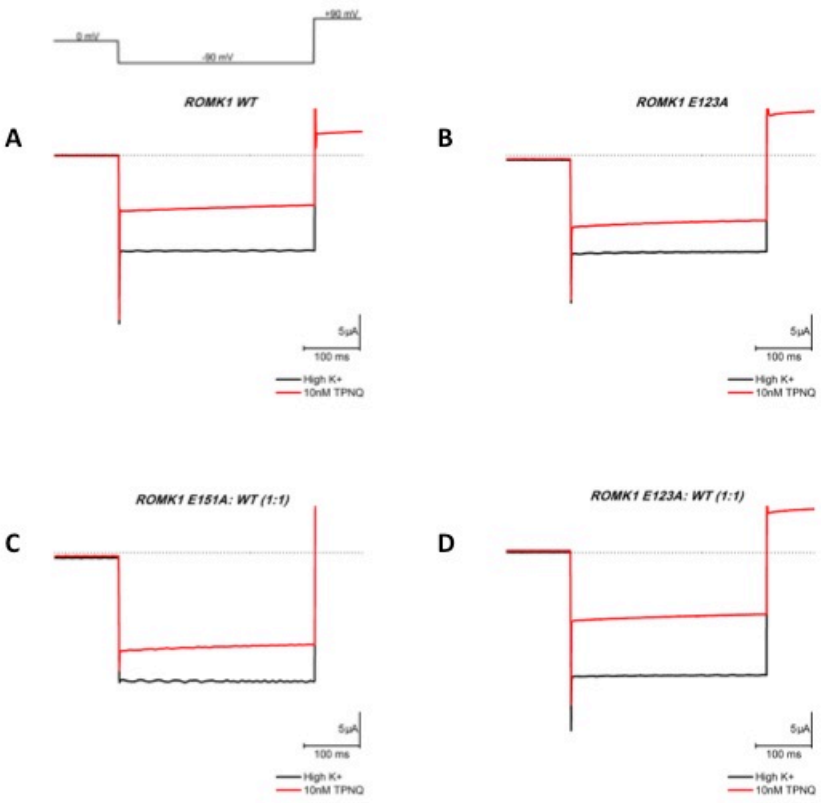

Figure 3. Inhibition of ROMK1 and its mutant channels by 10 nM TPNQ. Representative current traces of **A.** ROMK1 wild-type **B.** ROMK1 E123A mutant **C.** Coinjected ROMK1 E151A mutant **D.** Coinjected ROMK1 E123A mutant. Currents through the channels were elicited by stepping the membrane potential from the equilibrium potential (0 mV) to -90 mV and then to +90 mV for one-second intervals. The black current trace indicates the maximum basal current in ND96K (High K^+) solution and the red current trace indicates the remaining current in the presence of 10 nM TPNQ containing High K^+ solution. The ROMK1 mutant channels, E123A or E151A, are coexpressed with ROMK1 wild-type channels by coinjecting their cRNAs in one to one ratio. Dotted lines indicate the zero current levels.

Fig. 4

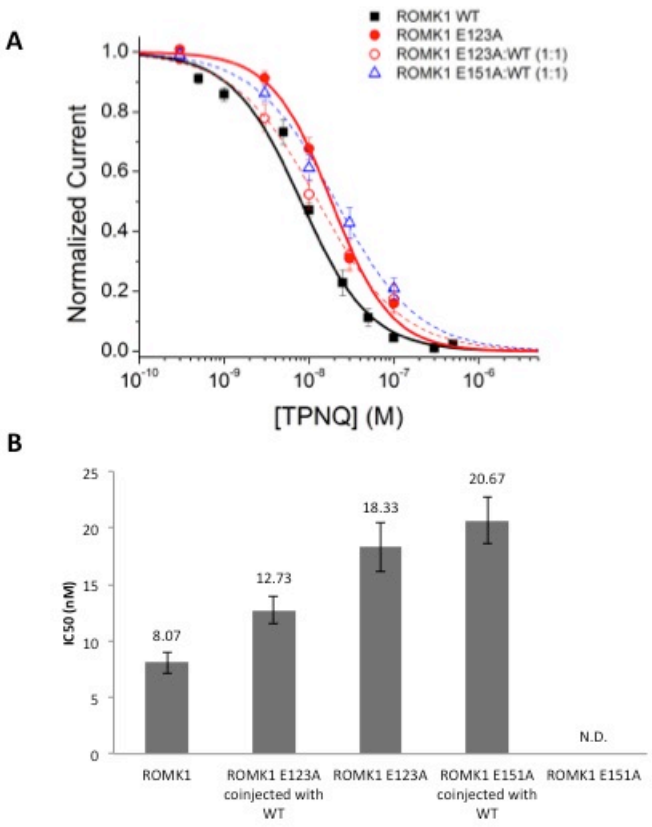

Figure 4. Summary comparison of TPNQ sensitivity of the ROMK1 wild-type and its mutant channels. A. Fraction of the unblocked channel currents (mean ± SEM., n ≥ 10) plotted against the TPNQ concentration. Leak currents, Barium insensitive currents, are subtracted from the each remaining current in the presence of various concentrations of TPNQ and then divided by the maximum basal currents in the absence of TPNQ in order to be normalized. The maximum basal currents were also subtracted from the leak currents prior to normalization. **B.** Summary bar graphs of IC_{50} values (mean ± SEM; N.D. indicates no detectable channel current). IC_{50} values were obtained using nonlinear curve fitting (Hill equation, see MATERIALS AND METHODS) based on the plots. Two sample t-tests were assessed to test for the significant difference in IC_{50} values of the ROMK1 mutant channels against the wild-type and also between two coinjected mutants (* indicates $p<0.05$, *** indicates $p<0.001$, n.s. indicates no significance).

TPNQ Sensitivities of the GIRK2 (Kir3.2) Wild-type Channel

Using the similar experimental conditions as in the previous ROMK1 studies, *Xenopus* oocytes were injected with *in vitro* transcribed mouse GIRK2 cRNA, and membrane currents were recorded 72-80 hours later using two-electrode voltage clamp (TEVC). In symmetrical 96 mM potassium solutions, ND96K (High K^+), the membrane was held at the equilibrium potential, namely at 0 mV. In order to elicit current through the channel, the same voltage step protocol was used, -90 mV and then +90 mV steps for one-second intervals.

In order to obtain the control for comparison studies with mutant channels, we first recorded the dose response of the GIRK2 wild-type channel to TPNQ. The IC_{50} was around 15 nM (Fig. 5). As described in a previous study (Yi et al., 2001), wild-type channels conduct small basal currents in High K^+ solution, in our hands the mean current was approximately -0.87 μA (Fig. 6A) including leak, endogenous currents insensitive to Barium Chloride block that ranged from -0.2 to -0.5 μA (data not shown). Hence, distinguishing such small basal currents from GIRK2 wild-type channel expression from the background endogenous currents was quite challenging.

Difficulties in Distinguishing the Basal Currents of the GIRK2 E127A Mutant from the Background Endogenous Currents

According to Sundaram's simulation studies on the TPNQ docked GIRK2 model (Fig. 2B), Glutamate 127 on all four subunits showed the highest interaction energy with the TPNQ residues: Arg7, Lys16, 17, 20, and 21. This model predicts that Glu127 is the main interacting residue on GIRK2 channel in direct-paired interactions with TPNQ.

Fig. 5 shows the dose-responses of GIRK2 wild-type channel and its E127A mutant channel to TPNQ. However, since the basal currents of E127A mutant channel were very small, even smaller than that of wild-type channel (data not shown), it was not possible to distinguish the basal currents of the mutant channel from the background endogenous currents. Therefore, we could not obtain strong evidence to conclude that the reduction in TPNQ sensitivity was that of this expressed GIRK2 mutant (Fig. 5).

Fig. 5

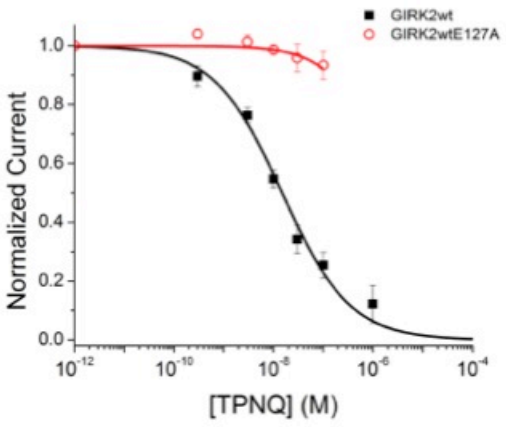

Figure 5. Inhibition of GIRK2 wild-type and its E127A mutant by TPNQ in a dose dependent manner. Fraction of the unblocked channel current of GIRK2 wild-type and its E127A mutant (mean ± SEM., n ≥ 4) plotted against the TPNQ concentration. The same normalization method was used as described in Fig. 4. Even though there was a decreasing trend against the various TPNQ concentrations shown in the Hill fitting in the GIRK2 E127A mutant, we could not confidently distinguish the true basal currents, ranging within a couple of hundred nA, from the background endogenous currents.

Fig. 6

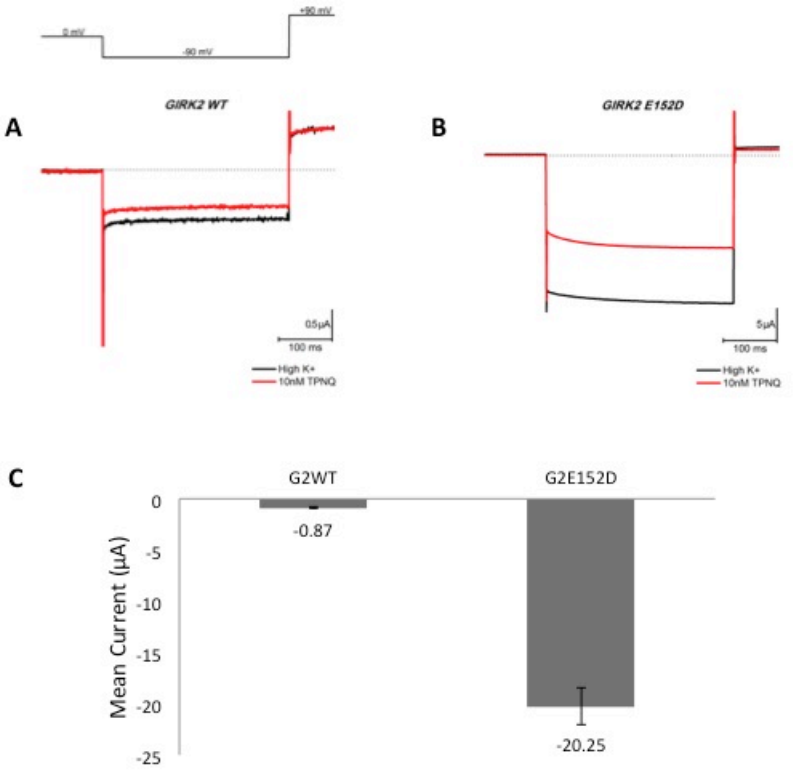

Figure 6. The E152D mutation enhances GIRK2 basal currents. Representative current traces of **A.** GIRK2 wild-type **B.** GIRK2 E152D. Currents through the channels were elicited with the same protocol described in Fig. 3. The black current trace indicates the maximum basal current in ND96K (High K^+) solution. The red current trace indicates the remaining current in High K^+ solution containing 10 nM TPNQ. Dotted lines indicate the zero current levels. **C.** Summary bar graphs of mean currents (mean ± SEM.). Approximately 20-fold enhancement in the basal currents is shown in the GIRK2 E152D current compared with that of the wild-type.

Thus, in an effort to enhance the currents of the mutant channel, we coinjected Gβγ cRNA. Gβγ has been shown to stimulate GIRK activity (Logothetis et al. 1987), and coexpression of $G\beta_1\gamma_2$ with GIRK subunits in *Xenopus* oocytes results in augmented currents (He et al., 1999). Fig. 8A clearly shows the enhancement in the basal currents of the GIRK2 wild-type channel by the Gβγ activation, while there appears to be no enhancement in the currents of the GIRK2 E127A mutant channel, which shows current levels similar to those of uninjected oocytes (Fig. 8B and E).

The GIRK2 E152D Mutant shows similar sensitivity to TPNQ as the wild-type channel

As previously described, these difficulties in distinguishing the basal currents of the mutant channels from the endogenous ones led us to use a pore helix mutant, GIRK2 E152D, previously reported to enhance basal currents by about 20-fold (Yi et al., 2001). Based on single-channel recordings, it was shown that this mutation did not affect the single-channel conductance but profoundly changed single-channel kinetics such as the increases in open probability and mean open duration (Yi et al., 2001). This indicates that the mutation enhances GIRK2 currents by changing its gating properties.

Large basal currents from expressed channels can be readily distinguished from endogenous background currents. Moreover, larger currents make it easier to detect changes in dose-response measurement. Therefore, if this pore helix mutant channel did not show any differences from the wild-type in TPNQ sensitivity, it could be used as a good representative of the GIRK2 wild-type channel in future studies with TPNQ.

Consequently, we examined the GIRK2 E152D channel under identical experimental conditions used for the GIRK2 wild-type channels to directly compare to each other. In agreement with previous studies (Yi et al., 2001), we also obtained dramatically enhanced basal currents, about 20-fold (-20.25 μA), compared with those from wild-type channels, (-0.87 μA) (Fig. 6C). Comparison of TPNQ sensitivity from dose-response experiments showed no significant differences between the GIRK2 wild-type and the E152D channel, IC_{50} = 14.82 nM and 18.3 nM, respectively (Fig. 7A and B).

Fig. 7

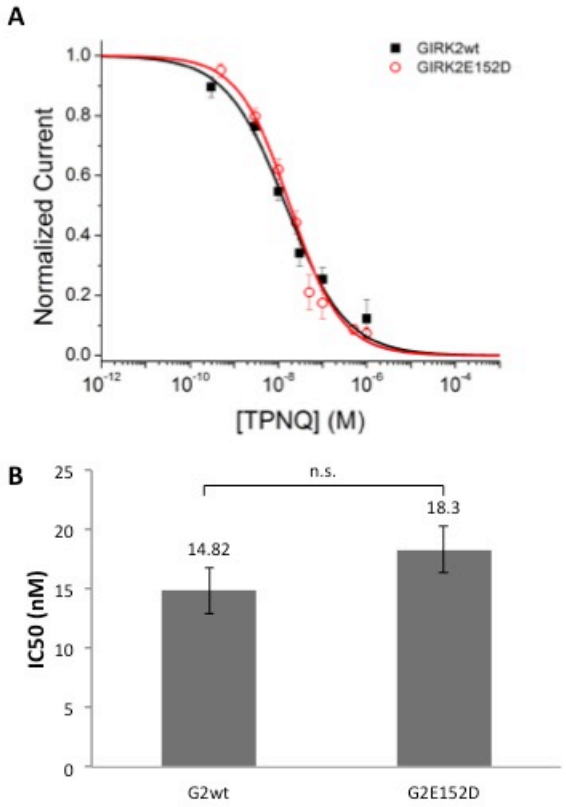

Figure 7. Similarity in TPNQ sensitivity between the GIRK2 wild-type and the GIRK2 E152D mutant. A. Fraction of the unblocked channel currents (mean ± SEM., n ≥ 4) plotted against the TPNQ concentration. The same normalization method was used as described in Fig. 4. **B.** Summary bar graphs of IC_{50} values (mean ± SEM.). IC_{50} values were obtained using the same Hill fitting as described in Fig. 4. Two sample t-tests for significance between IC_{50} values of GIRK2 and GIRK2 E152D channels (n.s. indicates no significance), which justify the GIRK2 E152D mutant as a substitute of the wild-type in the TPNQ studies.

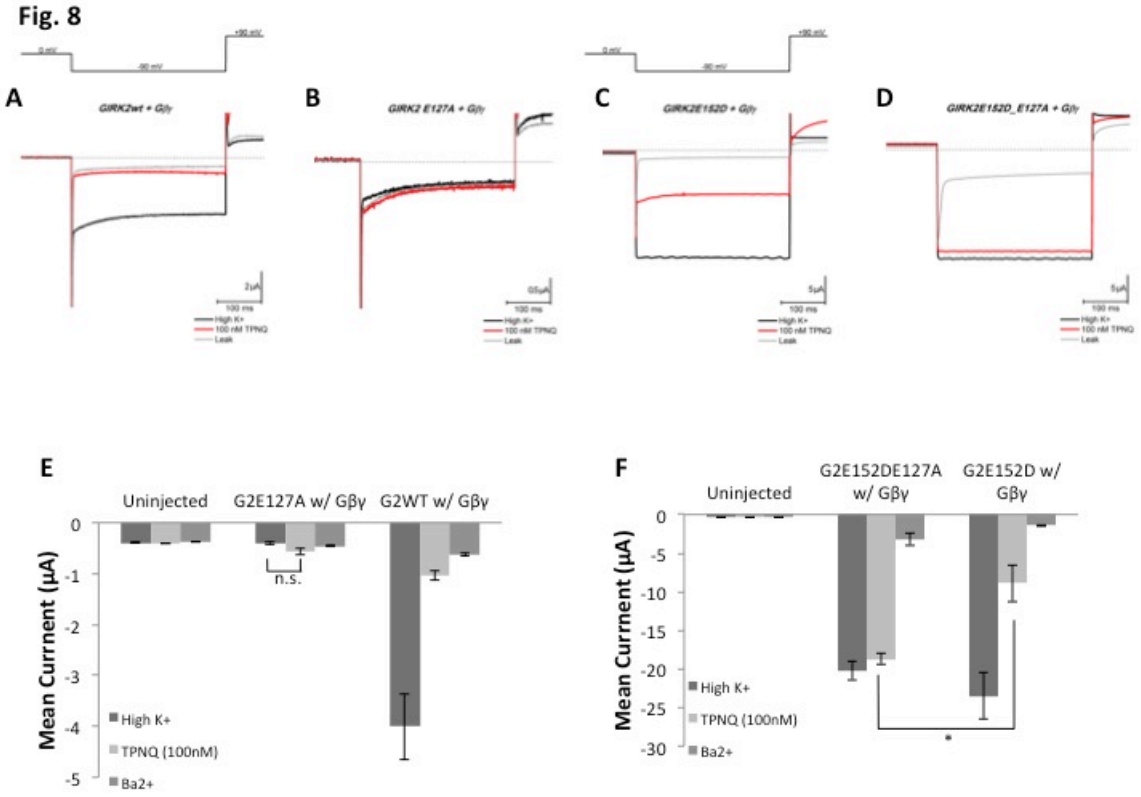

Figure 8. The basal current enhancement by the Gβγ activation on the homomeric GIRK2 and GIRK2 E152D in the presence and the absence of the E127A mutation. Representative current traces of **A.** GIRK2 wild-type **B.** GIRK2 E127A mutant **C.** GIRK2 E152D **D.** GIRK2 E152D_E127A mutant channels. All tested channels were coinjected with 2 ng of $G\beta_1$ and 2ng of $G\gamma_2$ cRNAs. Currents through the channels were elicited with the same protocol as described in Fig. 3. The black current trace indicates the maximum basal current in ND96K (High K^+) solution. The red current trace indicates the remaining current in High K^+ solution contaning.100 nM TPNQ. The grey current trace indicates the leak currents (currents remaining in the presence of 3 mM Barium Chloride). Dotted lines indicate the zero current levels. Summary bar graphs (mean ± SEM.) of the mean currents of **E.** GIRK2 wild-type and the E127A in the background of GIRK2 wild-type **F.** GIRK2 E152D and the E127A in the background of E152D, coexpressed with Gβγ. In both panels E and F uninjected oocytes were used as the negative control. Two sample t-tests were assessed to test for the significant difference between the mean currents of the GIRK2 E127A mutant in the presence of High K^+ solution and 100 nM TPNQ in panel E and between the mean currents of the GIRK2 E152D and the GIRK2 E152D_E127A in the presence of 100 nM TPNQ in panel F (* indicates $p<0.05$, n.s. indicates no significance).

Interestingly, Gβγ coexpression not only yielded huge measurable currents from the GIRK2 E152D_E127A mutant channel (Fig. 8D and F) but also showed a significant reduction of the TPNQ sensitivity of the E127A mutant channel (Fig. 8F).

Therefore, these data gave us confidence to consider the GIRK2 E152D mutant as a good representative of TPNQ sensitivity of the GIRK2 wild-type channel.

Effects of E127A mutation in the GIRK2 E152D background on TPNQ Sensitivity

Fig. 9A and B shows the current traces of GIRK2 E152D and its E127A mutant channel. There is about a 2-fold decrease in the mean current between the two channels, which suggests that the E127A mutation causes a reduction in the basal currents, -9.59 μA in the presence and -20.25 μA in the absence of the mutation (Fig. 9C). Moreover, as predicted by Sundaram's simulations (Fig. 2B) and shown in the Gβγ tests (Fig. 8F), the E127A mutation remarkably reduced the TPNQ sensitivity by greater than 10-fold. The IC_{50} for the channels in the absence and presence of the mutation are, 18.3 nM and 194.03 nM, respectively (Fig. 10A and B). This supports our prediction that the E127 is a critical residue in the paired residue interactions between the GIRK2 channel and TPNQ.

Effects of the GIRK1 subunits on the TPNQ sensitivity of GIRK2 channels

In another study from Lu's group (Ramu et al., 2004), chimeras between IRK1 with GIRK4 or GIRK1 were constructed to identify which subunits contribute to the high affinity inhibition of TPNQ on the heteromeric GIRK1/GIRK4 channels. These investigators concluded that GIRK4 subunits were the major ones contributing to the TPNQ sensitivity in the heteromeric channels.

We proceeded to conduct TPNQ dose-response studies with the heteromeric GIRK1/GIRK2 channels and predicted that the addition of GIRK1 subunits would reduce the TPNQ sensitivity of homomeric GIRK2 channels.

Fig. 9

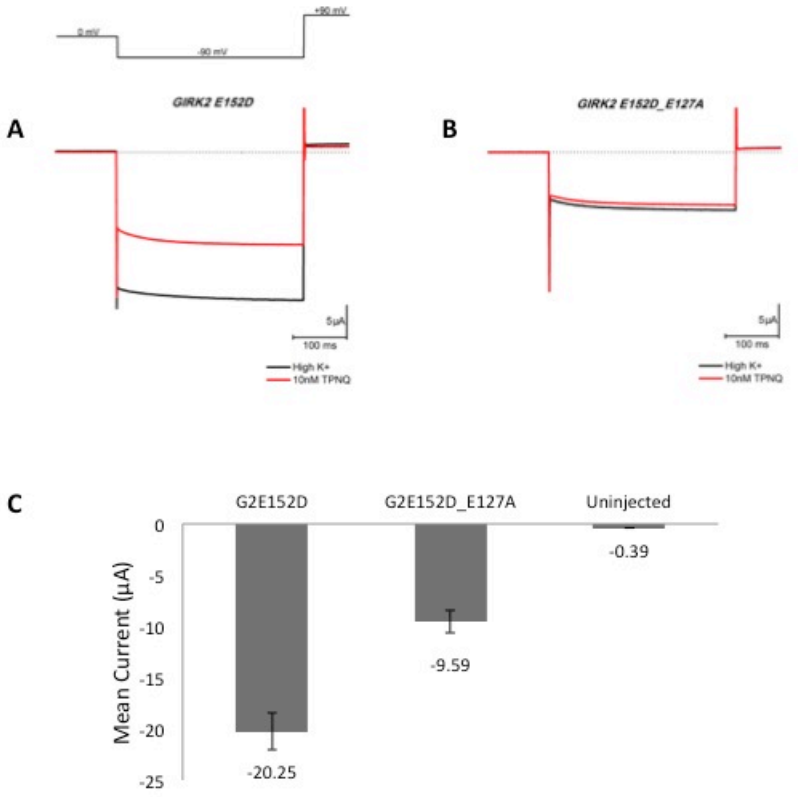

Figure 9. Reduction in the basal current by the E127A mutation in GIRK2 E152D channels. Representative current traces of **A.** GIRK2 E152D **B.** GIRK2 E152D with the E127A mutation. Currents through the channels were elicited with the same protocol as described in Fig. 3. The black current trace indicates the maximum basal current in ND96K (High K^+) solution. The red current trace indicates the remaining current in High K^+ solution containing 10 nM TPNQ. Dotted lines indicate the zero current levels. **C.** Summary bar graphs of mean currents (mean ± SEM.). Approximately 2-fold reduction was observed in the basal currents of GIRK2 E152D compared to the wild-type.

Fig. 10

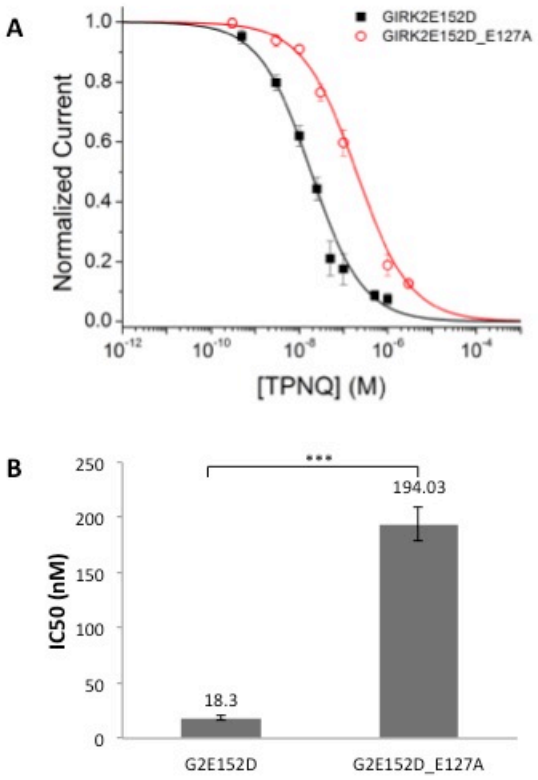

Figure 10. Effect of the E127A mutation on TPNQ sensitivity of Kir3.2 E152D channel. A. Fraction of the unblocked channel currents (mean ± SEM., n ≥ 4) plotted against the TPNQ concentration. The same normalization method was used as described in Fig. 4. **B.** Summary bar graphs of IC_{50} values (mean ± SEM.). IC_{50} values were obtained using the same Hill fitting as described in Fig. 4. Two sample t-tests were carried out to assess significant differences in IC_{50} values between the Kir3.2 E152D control and the E127A mutant (*** indicates $p<0.001$).

Fig. 11 shows the characteristic enhancement in the basal currents by the coexpression of GIRK1 and GIRK2 subunits as previously reported (Kofuji et al., 1995; Duprat et al., 1995; Velimirovic et al., 1996). We examined the TPNQ dose-response of heteromeric channels. Contrary to our hypothesis, there was no statistically significant difference in IC_{50} values between the homomeric GIRK2 and heteromeric GIRK1/GIRK2 channels, IC_{50} = 14.82 nM and 18.71 nM, respectively (Fig. 12A and B).

Effects of the GIRK1 on the TPNQ sensitivity of the heterotetrameric GIRK1/GIRK2 E127A mutant channels

We next tested the heteromeric GIRK1/GIRK2 channels with the E127A mutation; however, we failed to see detectable basal currents (data not shown). The Gβγ activation showed us a small but significant enhancement in terms of the current size in the basal current of the heteromeric GIRK1/GIRK2_E127A mutant channels (Fig. 13B and C), which confirms the presence of surface expression of the E127A mutant channels, whereas the heteromeric wild-type channels showed a large enhancement in the basal current (Fig. 13A and C). Again, these challenges in distinguishing basal currents of the E127A mutant channels from endogenous background ones led us to utilize the GIRK2 E152D channels.

Effects of the GIRK1 subunits on the TPNQ sensitivity of the heterotetrameric Kir3.1/Kir3.2 E152D channels

Fig. 14 shows the current traces of the homomeric and heteromeric GIRK2 E152D channels. The heteromeric GIRK1/GIRK2 E152D channels conduct much larger basal currents, -14.02 μA (Fig. 14 B and C) than the wild-type heteromeric GIRK1/GIRK2 channels do, -2.18 μA (Fig. 11B and C). In addition, the heteromeric GIRK1/GIRK2 E152D channels, IC_{50} = -17.81 nM, did not show a statistically significant difference in TPNQ sensitivity from the homomeric GIRK2 E152D channels, IC_{50} = -18.3 nM (Fig. 15A and B), a similar pattern to what we observed with the wild-type channels (Fig. 12A and B).

Fig. 11

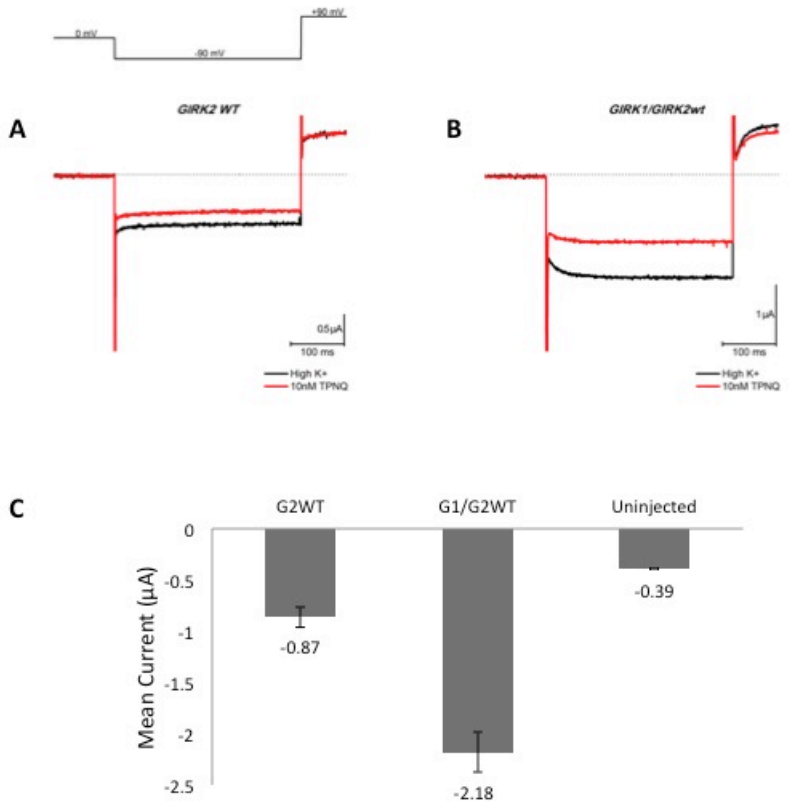

Figure 11. Characteristic enhancement in the basal currents by the coexpression of GIRK1 and GIRK2 subunits. Representative current traces of **A.** GIRK2 wild-type **B.** heteromeric GIRK1/GIRK2 channels. 2 ng of cRNA from each subunit were coinjected for coexpression. Currents through the channels were elicited with the same protocol as described in Fig. 3. The black current trace indicates the maximum basal current in ND96K (High K^+) solution. The red current trace indicates the remaining current in High K^+ solution containing 10 nM TPNQ. Dotted lines indicate the zero current level. **C.** Summary bar graphs of mean currents (mean ± SEM.). Approximately 2-fold increase in the basal currents was observed in the heteromeric GIRK1/GIRK2 compared with that of the homomeric GIRK2 channels.

Fig. 12

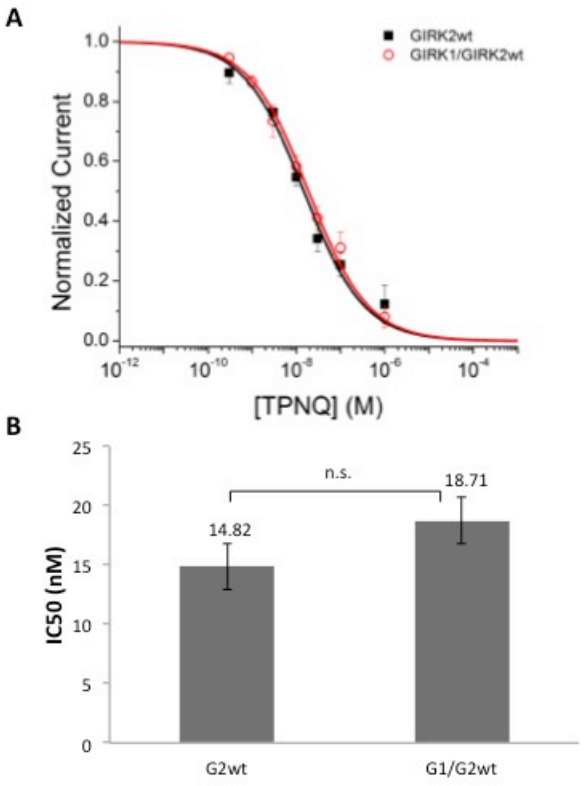

Figure 12. No significant decrease in the TPNQ sensitivity due to the addition of the GIRK1 subunits, TPNQ insensitive subunits, in the heteromeric GIRK1/GIRK2 wild-type channels. A. Fraction of the unblocked channel currents (mean ± SEM., n ≥ 4) plotted against TPNQ concentration. The same normalization method was used as described in Fig. 4. **B.** Summary bar graphs of IC_{50} values (mean ± SEM.). IC_{50} values were obtained using the same Hill fitting described in Fig. 4. Two sample t-tests were carried out to assess significant differences in IC_{50} values between the GIRK2 wild-type and heteromeric GIRK1/GIRK2 channels (n.s. indicates no significance).

Fig. 13

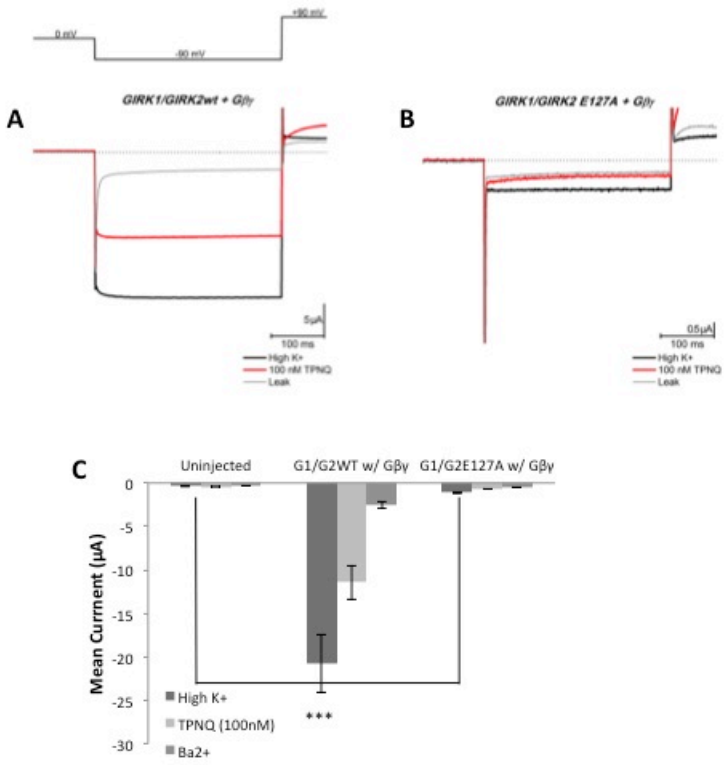

Figure 13. Basal current enhancement by coexpression of Gβγ with the heteromeric GIRK1/GIRK2 in the presence and absence of the E127A mutation. Representative current traces of **A.** the heteromeric GIRK1/GIRK2 wild-type **B.** the heteromeric GIRK1/GIRK2 E127A mutant channels. 2 ng of cRNA of each corresponding subunit were coinjected for coexpression. All tested channels were coinjected with 2 ng of $G\beta_1$ and 2ng of $G\gamma_2$ cRNAs. Currents through the channels were elicited with the same protocol as described in Fig. 3. The black current trace indicates the maximum basal current in ND96K (High K^+) solution. The red current trace indicates the remaining current in High K^+ solution containing 100 nM TPNQ. The grey current trace indicates the leak currents, currents remaining in the presence of 3 mM Barium Chloride. Dotted lines indicate the zero current levels. **C.** Summary bar graphs (mean ± SEM) of the mean currents of the channels. In panel C, uninjected oocytes were used as the negative control. Two sample t-tests were carried out to assess significant differences between the mean currents of the heteromeric GIRK1 with GIRK2 wild-type or the E127A mutant and uninjected oocytes (*** indicates $p<0.0001$).

Fig. 14

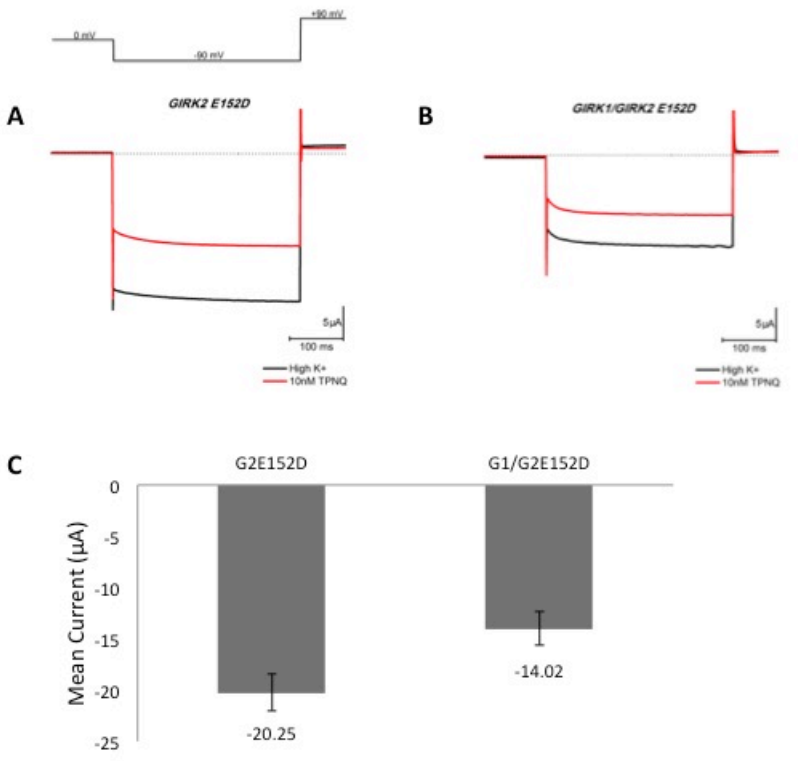

Figure 14. Mean currents of the coexpressed GIRK1 and GIRK2 E152D subunits. Representative current traces of **A.** GIRK2 E152D **B.** Heteromeric GIRK1/GIRK2 E152D channels. Currents through the channels were elicited with the same protocol as described in Fig. 3. The black current trace indicates the maximum basal current in ND96K (High K^+) solution. The red current trace indicates the remaining current in High K^+ solution containing 10 nM TPNQ. Dotted lines indicate the zero current level. **C.** Summary bar graphs of mean currents (mean ± SEM.).

Fig. 15

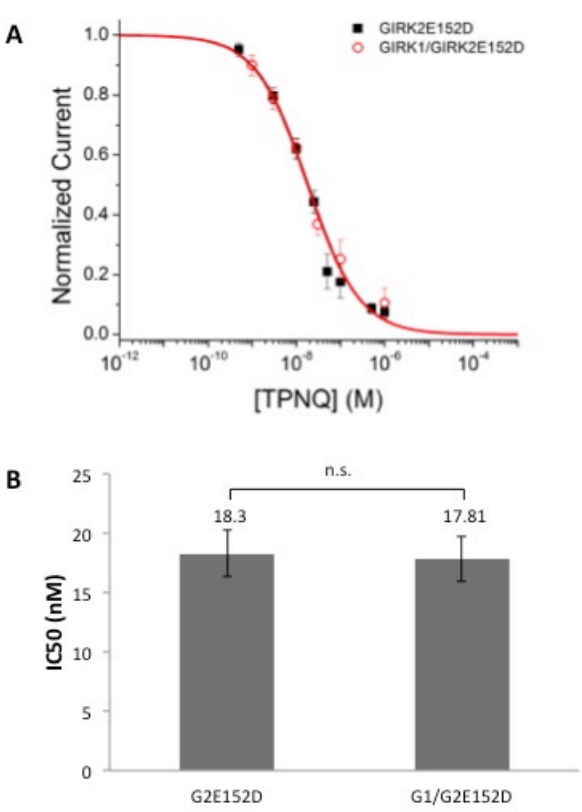

Figure 15. No significant decrease in the TPNQ sensitivity of GIRK2 E152D channels in the presence or absence of the TPNQ-insensitive GIRK1 subunits. A. Fraction of the unblocked channel currents (mean ± SEM., n ≥ 4) plotted against the TPNQ concentration. The same normalization method was used as described in Fig. 4. **B.** Summary bar graphs of IC_{50} values (mean ± SEM.). IC_{50} values were obtained using the same Hill fitting as described in Fig. 4. Two sample t-tests were carried out to assess significant differences in IC_{50} values between the GIRK2 E152D and the heteromeric GIRK1/GIRK2 E152D channels (n.s. indicates no significance).

Additional effects of the GIRK1 subunits and the E127A mutation on TPNQ sensitivity

Consequently, we conducted the TPNQ dose-response of the heteromeric GIRK1/GIRK2 E152D with E127A mutant channels. Fig. 16 shows examples of current traces of the homomeric and heteromeric GIRK2 E152D channels and their mutant channels. The reduction effect of the E127A mutation was also seen in the basal currents of the heteromeric GIRK1/GIRK2 E152D_E127A mutant channels, about a 2-fold decrease from the currents in the absence of the mutation (Fig. 16D).

Fig. 17 shows the summary of TPNQ sensitivity of the homomeric and heteromeric GIRK2 E152D channels and their E127A mutant channels. The TPNQ sensitivity of the heteromeric GIRK1/GIRK2 E152D_E127A mutant channels, IC_{50} = 317.77 nM, reflects the additive effects of the Kir3.1 subunits and the E127A mutation as compared with the homomeric GIRK2 E152D channels, IC_{50} = 18.3 nM. As the effect of adding the GIRK1 subunits, there is 1.7-fold decrease in TPNQ sensitivity between the homomeric GIRK2 E152D_E127A channels, IC_{50} = 194.03 nM, and their heteromeric channels, IC_{50} = 317.77 nM, though there are no statistically significant effects of GIRK1 subunits as the same patterns are consistently shown in the cases of the wild-type and E152D mutant channels. And as previously reported, there is a 10-fold decrease in the TPNQ sensitivity between the homomeric GIRK2 E152D and its E127A mutant channels, which reflects the effect of E127A mutation (Fig. 17B). Overall, an approximate 18-fold increase in IC_{50} values is shown in the heteromeric GIRK1/GIRK2 E152D_E127A compared with the homomeric GIRK2 E152D.

Fig. 16

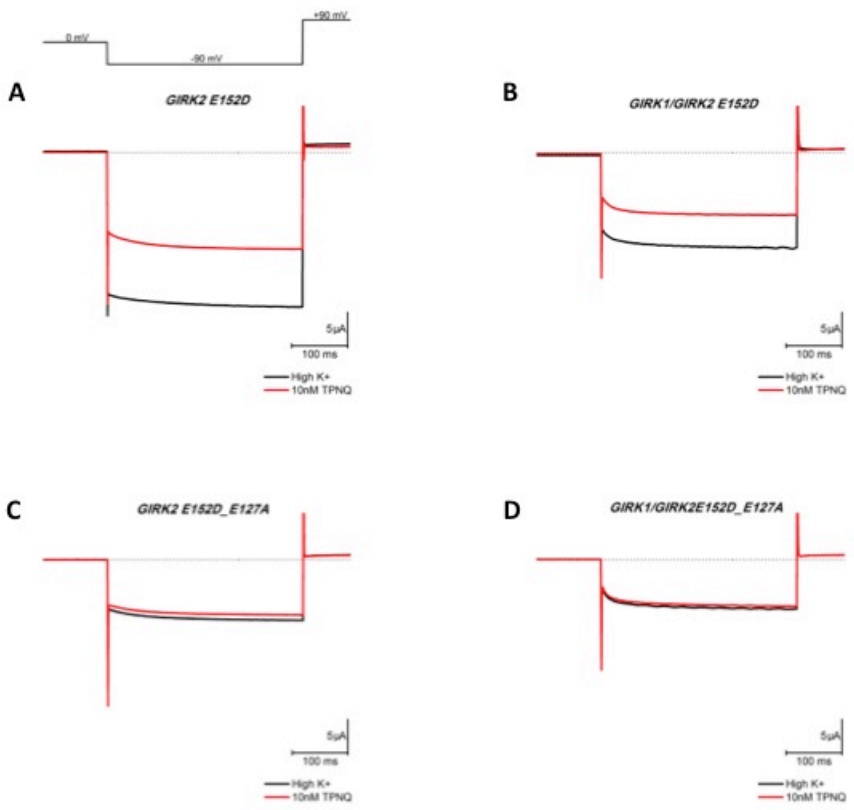

Figure 16. Examples of current traces that show the inhibition of the homomeric and the heteromeric GIRK2 E152D by 10 nM TPNQ in the presence and absence of the E127A mutation. Representative current traces of **A.** homomeric GIRK2 E152D **B.** Heteromeric GIRK1/GIRK2 E152D **C and D** in the presence of the E127A mutation of the channels in A and B, respectively. 2 ng of cRNA from each corresponding subunit was coinjected for coexpression. Currents through the channels were elicited with the same protocol as described in Fig. 3. The black current trace indicates the maximum basal current in ND96K (High K^+) solution and the red current trace indicates the remaining current in High K^+ solution containing 10 nM TPNQ. Dotted lines indicate the zero current level.

Fig. 17

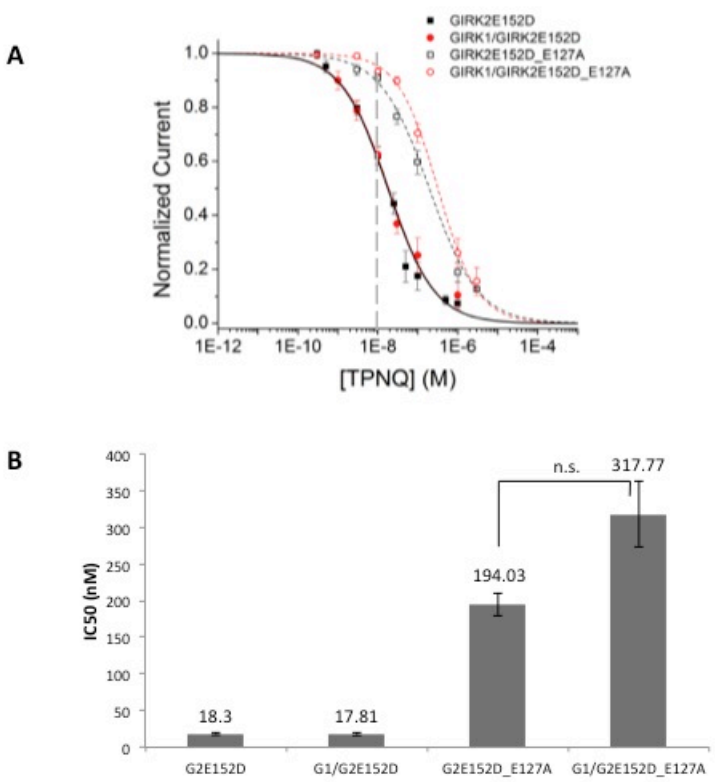

Figure 17. Additional effect of the GIRK1 subunits and the E127A mutation on TPNQ block of GIRK2 (E152D) currents. A. Fraction of the unblocked channel currents (mean ± SEM., n ≥ 4) plotted against the TPNQ concentration. Same normalization method was used as described in Fig. 4. **B.** Summary bar graphs of IC_{50} values (mean ± SEM). IC_{50} values were obtained using the same Hill fitting as described in Fig. 4. Two sample t-tests were carried out to assess significant differences in IC_{50} values between the homomeric GIRK2 E152D and the heteromeric GIRK1/GIRK2 E152D in the presence of the E127A mutation (n.s. indicates no significance). The grey dashed line indicates the remaining mean currents of the channels in the presence of 10 nM TPNQ. Additive effects are shown in the TPNQ sensitivity of the heteromeric GIRK1/GIRK2 E152D_E127A compared with that of the homomeric GIRK2 E152D. There is an approximately 18-fold difference between them, which appears to be contributed by the GIRK1 subunits (~1.7 fold) and the E127A mutation (10-fold).

DISCUSSION AND FUTURE DIRECTIONS

The goal of this study was to experimentally validate the predictions made by Sundaram's *in silico* alanine mutagenesis simulations of the TPNQ docked ROMK1_IRK2 (Fig. 2A) and GIRK2 models (Fig. 2B). The focus was on the specific paired residue interactions in order to test whether differences in the interaction energies could guide the design of specific TPN molecules to specifically block the channel of interest. In this study, we examined the relative contribution of two predicted residues, E123 and E151, in the ROMK1 and TPNQ. We also determined whether the pore helix mutant channel, GIRK2 E152D, previously reported to enhance basal currents (Yi et al., 2001) could serve as a good representative of the GIRK2 wild-type channel, particularly for TPNQ studies. Moreover, we determined the TPNQ sensitivity of the GIRK2 and the heteromeric GIRK1/GIRK2 channels in the dose-dependent manner to test the contribution of the GIRK1 subunits in the interaction of the heteromeric channel with TPNQ.

Consistent with previous reports (Jin et al., 1999) and computational predictions (Sundaram et al., unpublished), the homomeric ROMK1 E123A mutant channel showed a significant reduction in TPNQ sensitivity by more than 2-fold as compared to the wild type (Fig. 4A and B). Another predicted mutation, E151A, did not express detectable ionic currents, as previously reported by Lu's group (Jin et al., 1999). However, the coinjection method conferred the measurable currents of the coinjected E151A and wild-type channels. This indicates that there are heteromeric channels expressed with various combinations between the wild-type and E151A mutant subunits.

Furthermore, the coinjection method allowed us to directly compare the IC_{50} values of two coinjected mutant channels so that we could find out the relative contributions of each residue in the interaction between the ROMK1 and the TPNQ. Even though we might have expected a greater decrease in TPNQ sensitivity of ROMK1 by the E123A mutation than the E151A, since E123 has a greater number of high energy interactions with TPNQ residues than E151 (Fig. 2A), our results countered our expectations as there was no significant difference in the TPNQ sensitivity between the

two coinjected mutant channels (Fig. 3B). We may infer from the statistical results that E123 and E151 make a similar level of contribution to the paired interactions of ROMK1 with TPNQ.

According to alanine scanning mutagenesis studies by Lu's group (Jin et al., 1999), the effect of mutation of E123 was not particularly larger than mutations of other allosteric interaction sites. We suspected that the effect of our predicted mutations on binding interaction is probably compensated by the presence of several other strong allosteric interaction sites. We may test this by double mutating both residues and see how much of total interaction energies are contributed by the direct paired interactions.

We were able to see a much more remarkable effect of the predicted mutation, E127A (Fig. 2B), on the TPNQ sensitivity of the GIRK2 channels. However, we had to overcome a few experimental barriers. First, the basal currents of the GIRK2 wild-type were very small, ranging from -0.4 to -0.7 μA (data not shown), making it difficult to distinguish the true basal currents conducted by the target channel from the background endogenous currents, ranging from -0.2 to -0.5 μA (data not shown) and also hard to see the TPNQ inhibition of the channel in a dose-dependent manner.

The other problem was that the E127A mutation appeared to cause the reduction of the basal currents compared to wild-type controls. In both the homomeric GIRK2 wild-type and the heteromeric GIRK1/GIRK2 channels in the presence of the E127A mutation, the basal currents were not distinguishable from those of the uninjected oocytes (data not shown). In the case of the homomeric GIRK2 wild-type channels, the current was not detectable even with Gβγ stimulation (Fig. 8B and E; Fig. 13B and C), while the basal currents of both homomeric and heteromeric channels without the E127A mutation were dramatically increased by Gβγ stimulation (Fig. 8B). These Gβγ stimulation tests suggest that the E127A mutation affects the basal currents probably either by an effect on the surface expression or by affecting the gating properties of the channel.

In order to overcome the above experimental barriers, we examined a pore helix mutant GIRK2 E152D, previously reported to enhance basal currents by about 20-fold by altering only the channel gating properties (Yi et al., 2001). In our hands, this mutant also

dramatically enhanced basal currents by 20-fold compared with the wild-type channel (Fig. 6C). Also, the comparison of TPNQ sensitivity showed no significant difference between the GIRK2 wild-type and the E152D channels (Fig. 7A and B). Surprisingly, Gβγ stimulation produced large measurable currents of the GIRK2 E152D_E127A mutant channel (Fig. 8D and F) whereas there were almost no measurable basal currents in the GIRK2 E127A (Fig. 8B and E). The Gβγ stimulation tests also showed a remarkable effect on the TPNQ sensitivity of the E127A mutation. The inhibition of the GIRK2 E152D_E127A by 100 nM TPNQ was significantly reduced compared to the GIRK2 E152D (Fig. 8F). Therefore, the large basal currents and the similarity in the TPNQ sensitivity made the GIRK2 E152D mutant a good representative of the wild-type particularly for TPNQ studies.

Interestingly, further comparisons of the mean currents among homomeric and heteromeric GIRK2 E152D channels in the absence and presence of the E127A mutation showed a consistent 2-fold reduction of currents for E127A mutants (Fig. 9C; Fig. 16C and D). These results suggest that the E127A mutation caused a reduction in the basal currents probably by either altering the gating properties of the channel or reducing the surface expression level of the mutant channel.

Furthermore, as shown in Fig. 16, the ~2-fold reduction of basal currents in the GIRK2 E152D_E127A in both homomeric and heteromeric forms was not as dramatic as that of their wild-type ones, which showed almost no detectable basal currents even under Gβγ stimulation (Fig. 8B and E; Fig. 8B and C). This may indicate that the effect of the E152D mutation, which enhances the basal currents by altering gating properties, compensates for the reduction effect of E127A to some extent.

As predicted by the *in silico* studies, the TPNQ dose-dependence results from GIRK2 E152D_E127A showed a remarkable decrease, greater than 10-fold, in TPNQ sensitivity, which is consistent with the Gβγ stimulation studies (Fig. 8F). This supports our hypothesis that E127A is a critical interacting residue in the GIRK2/TPNQ interface, since it interacts with 5 residues on all four subunits (Fig. 2B) and is the one of the residues that reveals the largest effect of the mutation on TPNQ sensitivity.

We also tested the effect of adding GIRK1 (relatively TPNQ insensitive) subunits on the TPNQ sensitivity of GIRK2 subunits, since when both subunits are coexpressed they form heteromeric GIRK1/GIRK2 channels. Contrary to our expectation, the addition of the GIRK1 subunits did not significantly shift the TPNQ sensitivity from the homomeric GIRK2 (Fig. 12B). The GIRK2 in the background of E152D also showed no significant difference between the homomeric and the heteromeric channels (Fig. 15B), which offers another supportive piece of evidence to show its similarity to the wild-type. This implies that less than four GIRK2 subunits, are sufficient to confer a similar level of TPNQ sensitivity to what the four sensitive subunits can confer.

Interestingly, the additional effects of the E127A mutation and the GIRK1 subunits were found in the GIRK1/GIRK2 E152D with the E127A mutation (Fig. 17B). There was an approximate 18-fold increase in the IC_{50} values in the heteromeric GIRK1/GIRK2 E152D_E127A channel compared with the homomeric GIRK2 E152D channel. This may indicate that approximately a 1.7-fold increase in IC_{50} values was contributed by the GIRK1 subunits and about a 10-fold increase in IC_{50} values was contributed by the E127A mutation.

Earlier we considered that less than four sensitive subunits may be sufficient to confer TPNQ sensitivity at a level similar to that of homotetrameric channels. However, it appears that when the sensitive subunits lose critical residues, such as with the E127A mutation, which causes a further loss of TPNQ sensitivity, the effect of the Kir3.1 subunit is more pronounced as shown in the heteromeric GIRK1/GIRK2 E152D_E127A channel compared with the homomeric GIRK2 E152D channel.

Could we apply what we have learned from our study to design specific blockers for Kir channels? Knowing the interacting pairs of residues can serve as a strong starting point in designing specific blocker for Kir channels in terms of efficiency in the cost and labor. For example, if we wish to design a specific blocker that has higher selectivity for ROMK1 over GIRK2, we could synthesize substitutions in Arginine 7 and Lysine 20 of TPNQ to decrease its selectivity for GIRK2 since these residues do not appear to be critical for the ROMK1 interaction with TPNQ (Fig. 2). Or, if we wish to produce a blocker that is more selective for the GIRK2 over the ROMK1, we could decrease the

TPNQ sensitivity of the ROMK1 by substituting Lysine17 on TPNQ, since it interacts with two residues on ROMK1 that confer the two highest interaction energies while Lysine 17 with E127 of GIRK2 shows a relatively smaller interaction energy. The specific residue substitutions in TPNQ would be tested first *in silico* with our computational models to determine which residue substitutions would produce the best candidates to test experimentally.

However, the residues predicted by docking simulations (Sundaram et al., unpublished) change the TPNQ sensitivity only by 2-fold in ROMK1 E123A mutant and 10-fold in GIRK2 E127A mutant. To design a practical specific inhibitor, selectivity greater than 100-fold is required in order to achieve sufficiently selective inhibition of a target channel current (Ramu et al., 2008). Double mutation of TPN (H12L-M13Q), referred to as TPNLQ, made a toxin specific for ROMK1 over GIRK1/GIRK4 by greater than 250-fold (Ramu et al, 2008). This may suggest that we also need to select the residues that are interacting with the allosteric interaction sites and test more various combinations of substitutions to increase the selectivity.

This type of structure-function study suggests an efficient and cost effective way toward design and development of specific Kir channel blockers by focusing on specific paired interactions between TPNQ and the Kir channels.

LITERATURE CITED

Abraham MR, Jahangir A, Alekseev AE, Terzic A (1999) Channelopathies of inwardly rectifying potassium channels. *FASEB J.* 13:1901-1910.

Cannon SC (2007) Physiologic principles underlying ion channelopathies. *Neurotherapeutics* 4:174-183.

Corey S, Krapivinsky G, Krapivinsky L, Clapham DE (1998) Number and stoichiometry of subunits in the native atrial G-protein-gated K^+ channel, I_{KACh}. *J. Bio. Chem.* 273:5271-5278.

Dascal N, Schreibmayer W, Lim NF, Wang W, Chavkin C, DiMagno L, Labarca C, Kieffer BL, Gaveriaux-Ruff C, Troll- inger D (1993) Atrial G protein-activated K^+ channel: expression cloning and molecular properties. *Proc Natl Acad Sci* USA 90: 10235–10239.

He C, Zhang H, Mirshahi T, Logothetis DE (1999) Identification of a potassium channel site that interacts with G protein βγ subunits to mediate agonist-induced signaling. *J. Biol. Chem.* 274:12517-12524.

Ho K, Nichols CG, Lederer WJ, Lytton J, Vassilev PM, Kanazirska MV, Hebert SC. (1993) Cloning and expression of an inwardly rectifying ATP-regulated potassium channel. *Nature* 362: 31-38.

Jin W, Lu Z (1998) A novel high-affinity inhibitor for inward-rectifier K^+ channels. *Biochemstry* 37:13291-13299.

Jin W, Klem AM, Lewis JH, Lu Z (1999) Mechanisms of inward-rectifier K^+ channel inhibition by tertiapin-Q. *Biochemistry* 45:10129-10139.

Jin W, Lu Z (1999) Synthesis of a stable form of Tertiapin: A high-affinity inhibitor for inward-rectifier K^+ channels. *Biochemistry* 38:14286-14293.

Katz B. (1949) Les constants electriques de la membrane du muscle. *Arch Sci Physiol* 3: 285-299.

Krapivinsky, G., Gordon, E. A., Wickman, K., Velimirovic, B., Krapivinsky, L., and Clapham, D. E. (1995) The G-protein-gated atrial K^1 channel IKACh is a heteromultimer of two inwardly rectifying K^1 channel proteins. *Nature (London)* 374: 135–141.

Kubo Y, Miyashita T, Kubokawa K. (1993) A weakly inward rectifying potassium channel of the salmon brain. Glutamate 179 in the second transmembrane domain is insufficient for strong rectification. *J Biol Chem* 271: 15729-15735.

Lopatin AN, Makhina EN, Nichols CG (1995) The mechanism of inward rectification of potassium channels: “long-pore plugging” by cytoplasmic polyamines. *J Gen Physiol* 106: 923-955.

Matsuda H, Saigusa A, Irisawa H (1987) Ohmic conductance through the inwardly rectifying K channel and blocing by internal Mg2+. *Nature* 325: 156-159.

Ramu Y, Klem AM, Lu Z (2001) Titration of tertiapin-Q inhibition of ROMK1 channels by extracellular protons. *Biochemistry* 40: 3601– 3605.

Ramu Y, Klem AM, Lu Z (2004) Short variable sequence acquired in evolution enables selective inhibition of various inward-rectifier K^+ channels. *Biochemistry* 43:10701-10709.

Ramu Y. Xu Y, Lu Z (2008) Engineered specific and high-affinity inhibitor for a subtype of inward-rectifier K^+ channels. *Proc. Natl. Acad. Sci. USA* 105:10774-10778.

Sundaram S, Yang CH, Mahajan R, Logothetis DE (*in preparation*) Molecular Basis of the blocking mechanism of Inwardly Rectifying Potassium Channels by Tertiapin

Simon DB, Karet FE, Rodriguez-Soriano J, Hamdan JH, DiPietro A, Trachtman H, Sanjad SA, Lifton RP (1996) Genetic heterogeneity of Bartter's syndrome revealed by mutations in the K^+ channel, ROMK. *Nat Genet* 14: 152–156.

Sakmann B, Noma A, Trautwein W (1983) Acetylcholine activation of single muscarinic K+ channels in isolated pacemaker cells of the mammalian heart. *Nature* 303: 250-253.

Signorini S, Liao YJ, Duncan SA, Jan LY, Stoffel M (1997) Normal cerebellar development but susceptibility to seizures in mice lacking G protein-couple, inwardly rectifying K^+ channel GIRK2. *Proc. Natl. Acad. Sci. USA* 94:923-927.

Tao X, Avalos JL, Chen J, MacKinnon R (2009) Crystal structure of the eukaryotic strong inward-rectifier K^+ channel Kir2.2 at 3.1 Å resolution. *Science*. 326:1668-1674.

Whorton MR, MacKinnon R (2011) Crystal structure of the mammalian GIRK2 K^+ channel and gating regulation by G-proteins, PIP_2 and sodium. *Cell* 147(1):199-208.

Xu X, Nelson JW (1993) Solution structure of tertiapin determined using nuclear magnetic resonance and distance geometry. *Proteins* 17: 124-137.

Yang J, Yu M, Jan Y, Jan L (1995) Determination of the subunit stoichiometry of an inwardly rectifying potassium channel. *Neuron* 15: 1441-1447.

Yi B. A, Lin Y, Jan YN, Jan LY (2001) Yeast screen for constitutively active mutant G protein-activated potassium channels. *Neuron* 29:657-667.